Technical Notes

TECHNICAL NOTES are short manuscripts describing new developments or important results of a preliminary nature. These Notes cannot exceed 6 manuscript pages and 3 figures; a page of text may be substituted for a figure and vice versa. After informal review by the editors, they may be published within a few months of the date of receipt. Style requirements are the same as for regular contributions (see inside back cover).

Transonic Flowfield Past Two-Dimensional Airfoils between Porous Wind-Tunnel Walls

J.J. Kacprzynski*
National Research Council of Canada, Ottawa, Canada

MANY attempts have been made to evaluate the wind-tunnel wall corrections in the transonic regime; one of the more recent is that by Murman.[1] In this method a small-perturbation transonic equation is solved in a physical plane by the method of relaxation, assuming constant and identical porosity parameters for both the top and the bottom wind-tunnel walls. It has been known for quite a long time (e.g., Lukasiewicz[2] and, recently, Mokry[3]) that the porous wall characteristics are different for inflow from the plenum chamber to the test section than for outflow; hence they change along the wind-tunnel walls. Therefore, Murman's assumption of constant and identical porosity is a great simplification. Actually, the component of the velocity normal to the wind-tunnel wall is a nonlinear function of the difference of the static pressures on the wall and in the plenum chamber. This nonlinear characteristic is unknown, and, in the case of a porous wall, it is impossible to determine it purely experimentally. In the case of a slotted wall, the characteristics of the wall can be found by recording static pressures on both sides of the wall and the velocity distribution inside the slot.[4] The characteristic of the wall changes, not only with the Mach number, but also with Reynolds number (or with blowing pressure in pressurized wind tunnels).

One way of determining the effective porosity parameters of a porous wall is an inverse one, namely, from comparison of static pressure distributions on the porous wall obtained experimentally and theoretically for the assumed porosity parameters. Murman's method cannot be used directly for different porosities of the top and the bottom walls of the wind tunnel. Therefore, two other methods were developed for this purpose, the first one solving the small perturbation transonic equation in the physical plane, and the second one solving the full nonlinear transonic velocity potential equation in the Sells' plane. The methods were used, together with experimentally measured wall pressures, to establish by inverse means the effective wall porosity for a given experimental condition.

In the first method, the small-perturbation transonic equation is used. Putting the nonlinear term on the right-hand side, it can be written in the following form:

$$K\phi_{xx}+\phi_{\bar{y}\bar{y}}=(\gamma+1)\phi_x\phi_{xx} \tag{1}$$

where ϕ is the velocity perturbation potential, K the transonic similarity parameter, $\bar{y}$ the transformed y coordinate, and γ the ratio of specific heats. Assuming that the airfoil is located between two parallel walls (Fig. 1,) which are porous between points AB and DC, and constructing a Green's function satisfying homogeneous von Neumann boundary conditions on both walls, an analytic solution of Eq. (1) can be given in a symbolic form:

$$\phi(x,y)=-\int_A^B G\phi_{\bar{y}}dx+\int_D^C G\phi_{\bar{y}}dx+\int_{LE}^{TE}[G(\phi_{\bar{y}_b}-\phi_{\bar{y}_t})+G_{\bar{y}}(\phi_t-\phi_b)]dx+\int_{TE}^{\infty}\Gamma g_{\bar{y}}dx+\int_S\int(\gamma+1)\phi_x\phi_{xx}Gdxdy \tag{2}$$

where subscripts t and b denote top and bottom of the airfoil, LE and TE denote leading and trailing edge, and S is the area bounded by wind-tunnel walls. Γ is for the time being, an unknown circulation. It produces a discontinuity in the velocity potential in the wake behind the airfoil. G is Green's function. Assuming that the velocity potential is small far from the airfoil, the double integral over the surface S is evaluated only in the region bounded by $ABCD$. Equation (2) provides an analytical far-field solution and, hence, the values of the potential at lines AD and BC. The solution of Eq. (1) in the region bounded by the porous walls AB and DC and lines AD and BC is solved numerically with a relaxation method. In the iteration process, the value of circulation Γ and the values of the potential at lines AD and BC are updated every couple of iterations. The parameters determining the nonlinear character of the walls are guessed initially and verified by comparison of the experimental values of the static pressure along lines AB and DC with the calculated ones. This method was extended easily to account for airfoil boundary-layer effects by adding to the iteration process in region $ABCD$, a periodic boundary-layer calculation, with subsequent updating of the airfoil boundary condition by the addition of displacement thickness.

The present method easily can be modified for a case with porous walls extending from $-\infty$ to $+\infty$. It requires only a transformation of x coordinates is such a way that the infinite region of numerical calculation will be extended in physical x from $-\infty$ to $+\infty$. It is found that the value of the potential at lines AD and BC do not have to be calculated; values of the potential at these lines are given by the boundary condition at $\pm\infty$. The drawback of numerical calculations in the physical plane is the necessity of a large computer memory for storing values of the Green function. The advantage is the simplicity of accounting for viscous effects.

The second method developed for calculation of the transonic flow between porous wind-tunnel walls with nonlinear characteristics used the full nonlinear velocity potential equation.[5] The calculations are performed in the Sells' plane, namely, after mapping conformally the exterior of the airfoil, bounded by wind-tunnel walls, to the interior of a unit circle (Fig. 2). After the mapping, the airfoil contour is given by a circle and the walls by Fig. 8. The solution of the full nonlinear potential equation is performed as in the case of an infinite flow past an airfoil. The only modification is the replacement of the boundary condition at infinity by a boundary condition at the wall. This method is computationally more efficient than the previous one, but only for calculation of the inviscid flow. Calculations of the viscous flow in the Sells' plane represent some difficulty, because of modification of the camber of the airfoil and because of wake problems. In practice, it is used only for cases where the viscous effects can be approximated simply by a change in airfoil angle of attack.

Presented as Paper 75-81 at the AIAA 13th Aerospace Sciences Meeting, Pasadena, Calif., Jan. 20-22, 1975; submitted May 2, 1975; revision received Jan. 6, 1976.

Index category: Subsonic and Transonic Flow.

*Senior Research Officer. Member AIAA.

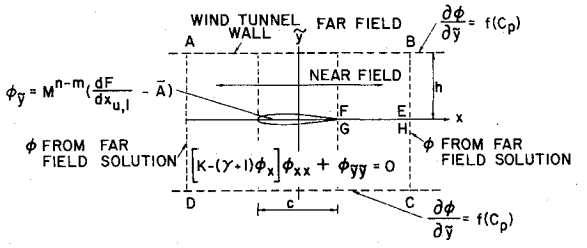

Fig. 1 Formulation of the problem in physical plane.

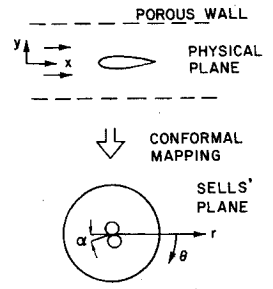

Fig. 2 Formulation of the problem in Sells' plane.

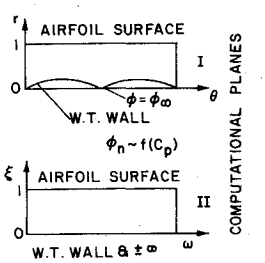

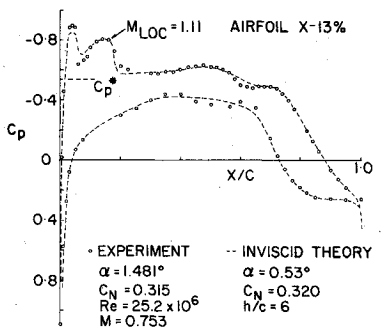

Fig. 3 Pressure distribution on the surface of the model.

For these cases, its high numerical efficiency allows for economical numerical experimentation in the determination of the effective porosity of wind-tunnel walls.

Calculated numerical examples past some airfoils, both contemporary supercritical ones and the conventional ones, show a very large influence of the wind-tunnel walls at transonic speed. Comparison of the flowfields past an airfoil between wind-tunnel walls and in free flow shows that these two flowfields are different, and that it is very difficult to eliminate the wind-tunnel wall effects.

An example of comparison of theoretical calculation with experiment is given for airfoil X-13%. It is a low-lift supercritical 13% thick airfoil, with a very blunt leading edge. In this case, the static pressure was recorded during the test just below ($\sim$2 in.) the ceiling and just above the floor ($\sim$2 in.). The height of the wind tunnel is 60 in. The ratio of the wind-tunnel height to the chord was $h/c=6$. The calculations were performed with the second method. Calculations of the viscous flow in the Sells' plane represent some additional difficulty because of the change of camber of the airfoil by the boundary layer, which requires updating the mapping functions. In order to avoid it, some special experimental cases were selected for comparison, cases for which viscous effects

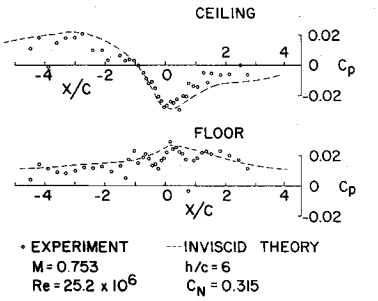

Fig. 4 Pressure distribution on the wind-tunnel wall at $Re=25.2\times10^6$.

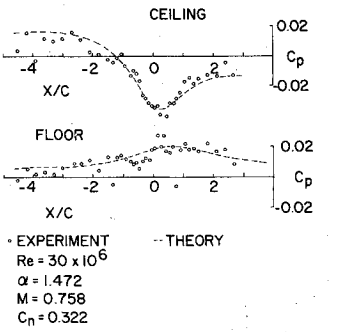

Fig. 5 Pressure distribution on the wind-tunnel wall at $Re=30\times10^6$.

should be approximated by the change of angle of attack only. In the presented case, the test was performed at Reynolds number $Re=25.2\times10^6$, Mach number $M=0.753$, and incidence $=1.481°$. The experimental normal force coefficient was $C_n=0.315$. In the numerical calculations, the angle, of attack was changed, and several values of the porosity parameters were tried in order to obtain agreement in normal force coefficients and in static pressure distributions on the wind-tunnel walls. Good agreement was obtained at $\alpha=0.53°$, with porosity parameters determined in the following way:

$$|V_{\text{normal}}|=A\cdot|C_p|+B\cdot C_p{}^2$$

with $A=0.25, B=7$ for $C_p<0$, and $A=0.08, B=2.3$ for $C_p>0$. The calculated normal force coefficient was 0.320. The pressure distributions agree well on both the airfoil (Fig. 3) and the wind-tunnel walls (Fig. 4). A small disagreement in the pressure distribuion on the upper surface, just near the leading edge, probably is due to bubble separation. The highest value of the local Mach number was 1.1, which does not create a strong shock wave/boundary-layer interaction.

It was observed that changing the Reynolds number did not change significantly the pressure distribution on the airfoil but changed the pressure distribution on the wind-tunnel walls. This can be explained partly as a viscous effect and partly as an effect of the change of the blowing pressure. An example of the pressure distribution on the wind-tunnel walls, at practically the same Mach number and incidence, but at higher Reynolds number, namely, 30×10^6, is shown in Fig. 5 for new values of the porosity parameters $A=0.4$, $B=10$ for $C_p<0$, and $A=0.05$, $B=1.5$ for $C_p>0$.

The two methods presented for calculation of transonic flowfields past airfoils in wind tunnels with porous walls decrease the disagreement between theory and experiment and enable the determination of the effective wall porosity, when measurements of the pressures along the walls are available. It clearly is evident from this limited study that the wall characteristics are nonlinear and are a function of a variety of parameters.

References

[1]Murman, E.M., "Computation of Wall Effects in Ventilated Transonic Wind Tunnels," AIAA Paper 72-1007, 1972.

[2] Lukasiewicz, J., "Effects of Boundary Layer and Geometry on Characteristics of Perforated Walls for Transonic Wind Tunnels," *Aerospace Engineering*, April 1961.

[3] Mokry, M., Peake, D.J., Bowker, A. J., "Wall Interference on Two-Dimensional Supercritical Airfoils, using Wall Pressure Measurements to Determine the Porosity Factors for Tunnel Floor and Ceiling," Rept. LR-575, Feb. 1974; National Research Council.

[4] Berndt, S.B., and Sorensen, H., "Flow Properties of Slotted Walls for Transonic Test Sections," AGARD Conference Proceedings No. 174, Wind Tunnel Design and Testing Techniques, London, Oct. 1975.

[5] Kacprzynski, J.J., "Transonic Flow Field Past 2-D Airfoils between Porous Wind-Tunnel Walls with Nonlinear Characteristics," AIAA Paper 75-81, 1975, Pasadena, Calif.

Application of the Measurement of Shock Detachment Distance at Low Supersonic Speeds

R.F. Starr* and M.O. Varner†
Arnold Engineering Development Center, Tullahoma, Tenn.

Introduction

THERE is currently an emphasis on accurate calibration of transonic and supersonic wind tunnels. This includes a precise definition of the spatial variation of flow properties in the test region as well as the fluctuation or temporal variation in flow properties. The shock detachment distance results given in the previous technical note[1] can be of more than academic interest since they demonstrate a very sensitive and repeatable variation with Mach number. A measurement of the shock detachment distance could be used to assess spatial and temporal flow quality independently of the other pressure and hot-wire techniques currently utilized.

Mach Number Resolution

The precision with which Mach number might be established from the shock detachment distance measurement must be addressed first. The variation of the shock standoff distance with Mach number taken from Fig. 3 of Ref. 1 is essential in establishing the resolution which might be achieved. In those aeroballistic range experiments, the standoff distance could be determined from the shadowgraph pictures to within 0.01 body diameters for a 1.5 in. diam sphere. The Mach number resolution that might then be expected in the wind tunnel at low supersonic speeds for this optimistic distance measurement precision and for a less optimistic precision is given in Fig. 1. Clearly the precision with which spatial Mach number variations could be measured in a transonic facility ($M_\infty < 1.2$) is acceptable and even comparable to that achieved with pressure systems. The absolute standoff distance could also be used to set tunnel Mach number precisely or to compare facilities in a fashion similar to the programs currently using other standard transonic bodies. As Mach number increases, the resolution deteriorates significantly based on these model size and precision assumptions.

Received August 29,1975; revision received December 8, 1975. The research reported herein was conducted by the Arnold Engineering Development Center (AEDC), Air Force Systems Command (AFSC), U.S. Air Force. Reseach results were obtained by personnel to ARO, Inc., contract operator of AEDC. Further reproduction is authorized to satisfy needs of the U.S. Government.

Index categories: Subsonic and Transonic Flow, Supersonic and Hypersonic Flow.

*Senior Engineer. Member AIAA.

†Research Engineer. Member AIAA.

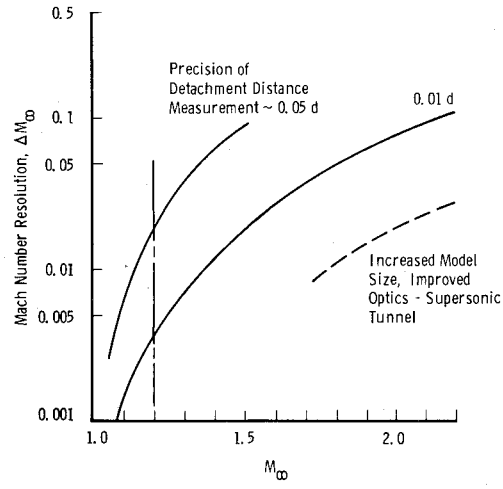

Fig. 1 Subjective analysis of Mach number resolution achievable with shock standoff distance technique.

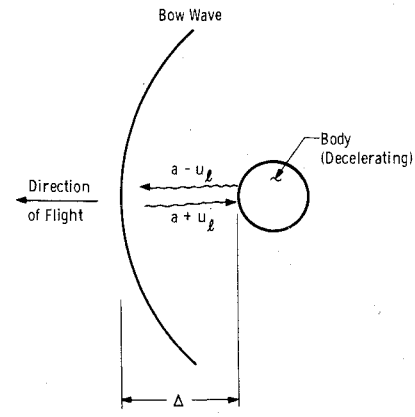

Fig. 2 Schematic of the aerodynamic communication process and resulting response time.

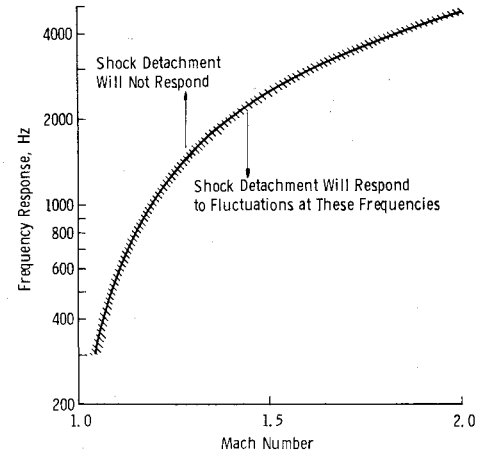

Fig. 3 Probable frequency response of shock detachment distance to flowfield oscillations.

However, model blockage constraints are not as dominant as the Mach number is increased, and the shadowgraph system of most supersonic tunnels is superior. This would permit a significant increase in model size and consideration of the more optimistic precision. Thus the resolution given by the dashed curve in Fig. 1 might be achieved near Mach 2.0.

Mach Number Fluctuations

The most promising application of this technique is the direct measurement of the Mach number fluctuation with